OXFORD GENETICS

GENETICS, 2023, iyad073
https://doi.org/10.1093/genetics/iyad073
Advance Access Publication Date: 21 April 2023
Investigation

Expression of retrotransposons contributes to aging in *Drosophila*

Blair K. Schneider,[1] Shixiang Sun,[2] Moonsook Lee,[2] Wenge Li,[3] Nicholas Skvir,[4] Nicola Neretti,[4] Jan Vijg,[2,5] Julie Secombe[1,6,*]

[1]Department of Genetics, Albert Einstein College of Medicine, 1300 Morris Park Ave., Ullmann 809 Bronx, NY 10461, USA
[2]Department of Genetics, Albert Einstein College of Medicine, 1301 Morris Park Ave., Price 468 Bronx, NY 10461, USA
[3]Department of Cell Biology, Albert Einstein College of Medicine, 1300 Morris Park Ave., Ullmann 909 Bronx, NY 10461, USA
[4]Department of Molecular biology, Cell biology and Biochemistry, Brown University, 70 Ship St., Providence 02903, USA
[5]Department of Ophthalmology and Visual Sciences, Albert Einstein College of Medicine, Bronx, NY 10461, USA
[6]Dominick P. Purpura Department of Neuroscience, Albert Einstein College of Medicine, Bronx, NY 10461, USA

*Corresponding author: Departments of Genetics and Neuroscience, Albert Einstein College of Medicine, 1300 Morris Park Ave, Bronx, NY 10461. Email: julie.secombe@einsteinmed.edu

Abstract

Retrotransposons are a class of transposable elements capable of self-replication and insertion into new genomic locations. Across species, the mobilization of retrotransposons in somatic cells has been suggested to contribute to the cell and tissue functional decline that occurs during aging. Retrotransposons are broadly expressed across cell types, and de novo insertions have been observed to correlate with tumorigenesis. However, the extent to which new retrotransposon insertions occur during normal aging and their effect on cellular and animal function remains understudied. Here, we use a single nucleus whole genome sequencing approach in *Drosophila* to directly test whether transposon insertions increase with age in somatic cells. Analyses of nuclei from thoraces and indirect flight muscles using a newly developed pipeline, Retrofind, revealed no significant increase in the number of transposon insertions with age. Despite this, reducing the expression of two different retrotransposons, *412* and *Roo*, extended lifespan, but did not alter indicators of health such as stress resistance. This suggests a key role for transposon expression and not insertion in regulating longevity. Transcriptomic analyses revealed similar changes to gene expression in *412* and *Roo* knockdown flies and highlighted changes to genes involved in proteolysis and immune function as potential contributors to the observed changes in longevity. Combined, our data show a clear link between retrotransposon expression and aging.

Keywords: lifespan extension, aging, retrotransposon, 412, Roo, Retrofind

Introduction

Across species, aging is associated with functional decline and an increased likelihood of one or more disorders that adversely affect quality of life (Dong *et al.* 2016; National Center for Health Statistics 2021). Driving the changes that occur at the whole animal level is a range of alterations to cellular function. One hallmark of aging is genomic instability, in which the accumulation of mutations can alter critical gene expression programs and impact cell division by promoting tumor formation or by increasing cellular senescence (López-Otín *et al.* 2013; Vijg and Suh 2013). One predicted genetic contributor to aging is the mobilization of transposable elements (TEs) in somatic cells. TEs are abundant, comprising ~45–50% of the human, ~37% of the mouse, and ~20% of the *Drosophila* genomes (Lander *et al.* 2001; Hoskins *et al.* 2002; Smith *et al.* 2007; McCullers and Steiniger 2017; Miao *et al.* 2020). While the specific TEs found in each animal species are distinct, they are a universal feature of eukaryotic genomes that are expressed in most cell types during aging (Pray 2008; De Cecco *et al.* 2013; Chen *et al.* 2016). Class 1 transposons, also known as retrotransposons (RTs), replicate using an RNA intermediate or a "copy, paste" mechanism (Pray 2008). RTs are therefore able to increase their genomic copy number over time, which gives them a high mutagenic potential. In contrast, class 2 transposons (DNA transposons) mobilize by excising themselves in a "cut, paste" mechanism, so their total number does not increase over time (Pray 2008). However, the precise role that TEs play in driving age-related phenotypes remains an open question.

The most obvious consequence of TE expression with age is the potential to cause genomic instability through insertional mutagenesis and/or the creation of insertions or deletions because of the double-stranded DNA breaks that are needed for TE reinsertion (Pray 2008; Levin and Moran 2011). In some contexts, TE expression increases with age; however, less is known about the impact of TE insertions on the aging process (Pray 2008; De Cecco *et al.* 2013; Chen *et al.* 2016). In addition, cDNA generated as an intermediate during RT mobilization can activate the immune response and lead to chronic inflammation in mammals (De Cecco *et al.* 2019; Simon *et al.* 2019; Miller *et al.* 2021). Consistent with their potential for interfering with cellular function, several mechanisms that are conserved across species have evolved to limit the expression of transposons. For example, many transposons in the genome are contained within constitutive heterochromatin, which is largely transcriptionally silent (Smith *et al.* 2007; Li *et al.* 2013; Vijg and Suh 2013; Gorbunova *et al.* 2014; Janssen *et al.* 2018; Gorbunova *et al.* 2021). For those

Received: December 12, 2022. **Accepted:** April 11, 2023

elements inserted within euchromatin, RT expression is regulated post transcriptionally via the siRNA pathway that degrades double-stranded RNA complexes (Wang *et al.* 2010; Sioud 2021). Further supporting a role for heterochromatin and RNAi in repressing the influence of TEs on aging, modulating the activity of either of these pathways can alter lifespan. For example, reducing the expression of the heterochromatin component *Lamin B*, or components of RNAi-mediated TE silencing machinery, decreases lifespan in *Drosophila* (Li *et al.* 2013; Chen *et al.* 2016). Conversely, increasing expression of the heterochromatin-promoting histone methyltransferase *su(var)3-9*, or the activity of the RNAi pathway, extends lifespan (Li *et al.* 2013; Wood *et al.* 2016; Yang *et al.* 2022). It is, however, notable that heterochromatin and the RNAi pathway are not specific to the repression of TEs, which complicates the interpretation of the changes to lifespan observed. More direct evidence supporting a link between TE activation and aging has come from the use of reverse transcriptase inhibitor drugs that broadly inhibit the ability of RTs to replicate. For example, *Drosophila* fed nucleoside reverse transcriptase inhibitors (NRTIs) have an increased lifespan compared to controls (Driver and Vogrig 1994). This is also observed in mice, where NRTI treatment attenuates the shortened lifespan caused by loss of *SIRT6*, a repressor of *LINE1 (L1)* elements (Simon *et al.* 2019).

The key to understanding the link between TEs and aging is defining the extent to which their expression leads to new insertions. Analyses of the TE *mdg4* (formerly known as *Gypsy*) in the adult *Drosophila* brain and fat body using a reporter revealed an increase in the number of insertions with age (Li *et al.* 2013; Wood *et al.* 2016; Chang *et al.* 2019). However, expanding these findings to endogenous TEs has been challenging, as each somatic cell contains a unique set of insertions which are difficult to detect using bulk whole genome sequencing (WGS) approaches. One approach to address this has been to develop bioinformatic tools to detect TE insertions more accurately, for example, by using TE junction and target site duplication (TSD) data. When applied to bulk WGS, this approach can detect an age-associated increase in TE insertion number in fly strains with reduced RNAi pathway activity and in clonally expanded tumors, but not in wild-type animals (Siudeja *et al.* 2021; Yang *et al.* 2022). New insertions can also be identified using long-read sequencing of bulk DNA as whole elements are detected rather than breakpoints (Siudeja *et al.* 2021; Yang *et al.* 2022). While a small number of de novo insertions were observed using this technique, it was difficult to determine how frequently TEs mobilized. While technologies to detect new TE insertions in somatic cells have become more robust using bulk sequencing approaches, the frequency of new TE insertions within individual somatic cells during aging remains unknown.

To understand the extent to which TEs mobilized during aging, we took a single nucleus WGS approach using a new pipeline called Retrofind that allows us to accurately define the insertional position and load per cell. Using nuclei isolated from adult thoraces or indirect flight muscles (IFMs), we found that the number of TE insertions does not increase with age. However, reducing the expression of two individual TEs, *412* and *Roo*, led to lifespan extension. This suggests a key role for the expression, and not insertion, of TEs impacting lifespan. This increased lifespan did not correlate with improved stress resistance or other health improvements traditionally associated with longer life. Transcriptomic studies of long-lived TE knockdown flies revealed that the expression of genes involved in proteolysis were upregulated, including the *Jonah* family of genes that encode serine hydrolases. Additionally, antimicrobial peptides (AMPs), the downstream products of activation of the *Drosophila* innate immune system that is similar to mammalian inflammation, were dysregulated in knockdown animals. Overall, our studies show that TE expression and not insertion likely contributes to aging, potentially through regulation of the *Jonah* genes and immunity.

Materials and methods

Fly strains

The following fly stocks were obtained from Bloomington Drosophila Stock Center: Act5C-Gal4 (BL #3954), w^{1118} (BL#5905), UAS-dcas9-VPR (BL#67062). UH3-Gal4 was a gift from the Sparrow lab (Singh *et al.* 2014). UAS-shRNAs were generated according to the TRiP protocol using the pVALIUM20 vector (Addgene) (Perkins *et al.* 2015). shRNA primers are listed in the primers table and were designed using the Designer of Small Interfering RNA webtool (Vert *et al.* 2006). UAS-shRNA transgenes were inserted into the attP site at 86F (BL #24749) by BestGene. gRNA flies for CRISPR interference (CRISPRi) were generated using the protocol from CRISPR fly design (Port *et al.* 2014; Akbari *et al.* 2015; Port *et al.* 2015; Port and Bullock 2016; Heigwer *et al.* 2018; Port *et al.* 2020a; Port *et al.* 2020b). The pCFD3 vector (Addgene) was used to insert a gRNA downstream of the U6:3 promoter that drives for ubiquitous expression of the gRNA. gRNA transgenes were inserted into the attP site at 86F (BL #24749) by BestGene. UAS-dcas9:KRAB flies were created by In-Fusion® cloning system (Takara) using the pUAST-attB vector from the Drosophila Genomics Resource Center (# 1419) and dCas9-KRAB (Addgene SID4X-dCas9-KRAB; #106399). The primers are listed in Supplementary Table 1, and the PCR amplifications were performed using the CloneAmp™ HiFi PCR Premix (Takara). The pUAST-dCas9-KRAB plasmid was recombined into the attP site attP40 (BL #24749) by BestGene.

Fly care

Fly food contained 80 g malt extract, 65 g cornmeal, 22 g molasses, 18 g yeast, 9 g agar, 2.3 g methyl para-benzoic acid, and 6.35 ml propionic acid per liter. Flies were kept at 25°C with a 12-hour light/dark cycle and 50% humidity. w^{1118} flies used for age-associated TE expression data were kept at room temperature (~22°C). Day of eclosion is defined as day 0 in all analyses. Adults were collected 2 days after the first flies eclosed, allowed to mate for a day, sorted by sex, and allowed to age to the specified time point. Flies were kept at a density of 25 or less per vial. Flies were transferred to a new vial of food twice a week until they reached the desired age for the experiment. All studies presented used female flies.

RNA-Seq

Triplicate samples of 20 thoraces from adults were collected at day 20 from Act5C > shRNA (Control, 412#1, and Roo) and frozen at −80°C. RNA was extracted using TRIzol (Invitrogen) and sent to Novogene for quality assessment, library preparation, sequencing, and differential expression analysis. Sequencing was performed on an Illumina platform. HISAT2 was used to map the reads to the *Drosophila* genome (*dm6*), Novogene calculated the read counts and FPKM (fragments per kilobase of transcript per million base pairs sequenced) values and then used DESeq2 to perform differential expression analysis (Kim *et al.* 2019). DAVID was used to obtain gene ontology (GO) terms (Huang da *et al.* 2009; Sherman *et al.* 2022). String was used to highlight the functional relationships of the enriched gene products (Szklarczyk *et al.* 2021). Data generated have been deposited in NCBI's Gene

Expression Omnibus (Edgar *et al.* 2002) and are accessible through GEO Series accession number GSE207160.

qPCR

TRIzol was used to extract total RNA from 5 whole adult flies to quantify knockdown efficiency. To examine expression of TEs in young and old flies RNA was extracted from 8 thoraces. RNA was DNase treated (Invitrogen), and cDNA was synthesized using the Verso cDNA kit (Thermo-Fisher AB1453A). One to five micrograms of RNA was used for cDNA synthesis. PowerUp SYBR Green Master Mix was used to perform qPCR on the Applied Biosystems QuantStudio3 system. *rp49* (*RpL32*) was used as the housekeeping gene to normalize relative gene expression changes. Experiments were performed in 3–5 biological replicates. An unpaired t-test with Bonferroni correction was used as the statistical test. Primers used in these experiments can be found in Supplementary Table 2 (Kalmykova *et al.* 2005; Czech *et al.* 2008; Ghildiyal *et al.* 2008; Dufourt *et al.* 2014; Matsumoto *et al.* 2015; Chen *et al.* 2016; Hur *et al.* 2016; Klein *et al.* 2016; Drelon *et al.* 2019).

Lifespan quantification

Adult flies were collected 48 hours after eclosion and mated for 24 hours. Female flies were then placed at a density of no more than 25 flies per vial. The number of dead animals was counted twice a week and remaining live flies were transferred to new food vials. Lifespan experiments were performed in triplicate (separate crosses) and results pooled. A Dunnett test was used to compare survival curves. A Gehan-Breslow-Wilcoxon test was used to compare median lifespan. Difference in maximum lifespan was calculated by a permutation test (95th percentile) followed by a two-sided t-test with correction for multiple comparisons.

Oxidative stress survival

Flies were placed on 20 mM paraquat (Sigma), 1% agar, 5% sucrose media at day 40 post eclosion. The number of dead animals was counted every 4–8 hours until no live flies remained. The experiment was performed in biological triplicate. A Dunnett test was used to compare survival curves.

Starvation survival

Day 40 adult flies were provided with Whatman paper-soaked in water and the number of dead animals counted every 4 hours until all flies were dead. The experiment was performed in biological triplicate. A Dunnett test was used to compare survival curves.

Endoplasmic reticulum stress survival

Flies were placed on 12 μM tunicamycin (Sigma), 1.5% agar, and 5% sucrose media at day 20 post eclosion and survival quantified. The experiment was performed in biological triplicate. A Dunnett test was used to compare survival curves.

Negative geotaxis

Flies at days 5, 20, and 40 post eclosion were recorded while they were tapped down to the bottom of empty vials. After 10 seconds, the number of flies in each third of each vial were counted. Flies were allowed a minute to recover before the experiment was repeated. The experiment was performed a total of three times in biological triplicate. A Chi-square test for trend was used to compare the locomotor activity of the different genotypes.

Fecundity and fertility

Females were mated with w^{1118} males (1:1 ratio) at day 25 post eclosion at a density of approximately 20 flies per vial. Females were given 24 hours to lay eggs, then transferred to a new vial and the eggs per vial were counted every day for 5 days. Fecundity was calculated as the average number of eggs laid per vial per day. To assess fertility, the number of eggs laid was quantified and animals allowed to develop until eclosion at which point the number of adults flies was quantified. The fertility index was calculated by dividing the number of adult flies by the number of eggs laid per vial. A fertility index of 1 is defined as 100% fertile. A One-way ANOVA was used to calculate the differences in fecundity and fertility across genotypes.

Thermal stress survival

To test sensitivity to cold stress, flies were placed in new food vials and placed at 4°C on ice for 15 hours at day 20 post eclosion. Flies were given 48 hours to recover at 25°C and the number of dead flies were counted. To test heat sensitivity, flies were placed in new food vials and placed at 37°C until about 80% of flies were immobile at the bottom of the vial with heat paralysis. Flies were given 48 hours to recover at 25°C, and the number of dead flies were counted. Assays were performed in biological triplicates. Fisher's exact test was used to calculate the difference in survival across genotypes.

Body weight and animal size

Zeiss Discovery.V12 SteREO with the AxioVision Release 4.8 software was used to capture pictures of adult flies using a ruler to show size. All images were processed using Adobe Photoshop. Flies were 2 days post eclosion for imaging and body mass quantification. To measure body mass, 10 flies of each genotype were placed in 1.5 mL Eppendorf tube and weighed. This was done in biological triplicate. A one-way ANOVA was used to calculate body weight differences across genotypes.

Bacterial infection survival

Flies were challenged with bacterial infection using *Bacillus subtilis* (ATCC 6051™) at day 20 of age. *Bacillus* was grown on LB plates/media at 35°C to a density of $1.25X10^{11}$ CFU/mL colony forming units (CFUs) similar to a published protocol (Chatterjee *et al.* 2016). CFUs were calculated according to (Allen). Flies were anesthetized with CO_2 and then infected with bacteria. A tungsten needle (Fisher) was dipped in the bacterial culture or PBS for sham infection control. Flies were placed back in food vials and allowed to recover. Dead flies were counted every 24 hours and survival was calculated per genotype. This experiment was performed in biological triplicate (~20 flies per vial). A one-way ANOVA was used to compare survival across genotypes and an unpaired t-test with Bonferroni correction was used to compare the bacterial infected flies in each genotype to their sham control.

Purification and amplification of individual thoracic nuclei

Forty to 60 thoraces from young (5 days old) or old (50 days old) w^{1118} flies were dissected and single nuclei were prepared according to (Corces *et al.* 2017) with minor alterations. Briefly, instead of using a Polytron, thoraces were homogenized with an automatic pestle for 5 minutes on ice, transferred to a 7 mL Dounce homogenizer, and pulverized with 30 stokes of the pestle. Debris was filtered using a 20-micron filter and subsequently with a 10-micron filter (twice). Nuclei were then sorted into individual

tubes using the CellRaft AIR® System (Cell Microsystems). Genomic DNA from each nucleus was amplified by multiple displacement amplification (MDA). The resulting amplicons were used to make sequencing libraries according to (Dong *et al.* 2017). Libraries (21 per group) were subjected to paired end WGS on the Illumina 2500 platform at Novogene. The data were deposited in NCBI's Sequence Read Archive and are accessible through BioProject accession number: PRJNA854389.

Purification and genome amplification of IFM nuclei

UH3-Gal4/+; +/+; UAS-Klar-KASH/+ flies were aged to either 5 (young) or 60 (old) days. 50 thoraces per group were dissected and single nuclei were prepared using the nuclei EZ isolation kit (Sigma) according to manufacturer instructions. Nuclei were then stained with 4′,6-diamidino-2-phenylindole (DAPI) and subjected to fluorescence-activated cell sorting (FACS), gaiting for DAPI and GFP-positive populations using the MoFloXDP at the Flow Cytometry Core Facility at Albert Einstein College of Medicine. The first gate selected for size by plotting forward scatter (FSC, size) against side scatter (SSC, granularity), with debris being outside the gate. 99.6% of the population was not debris. A log scale was used to visualize high signals from both axes in the same plot. The second gate selected for single nuclei by plotting SSC-width (doublets) against SSC-height (intensity). Single nuclei were 30.14% of the population. The last and final gate selected for intact IFM nuclei by plotting GFP (IFM) against DAPI (DNA). The nuclei were sorted into individual tubes and subjected to MDA using the REPLI-g® UltraFast Mini kit (Qiagen) as described (Gundry *et al.* 2012). Bulk/pooled unamplified genomic DNA from young abdominal segments was used as the control for genomic insertions already present in the strain. Data was deposited in NCBI's Sequence Read Archive and is accessible through BioProject accession number: PRJNA854818.

Analyses of transposon insertions

Fastq files were analyzed using the new pipeline Retrofind and the published pipeline from the Bardin lab (Siudeja *et al.* 2021). Retrofind pre-filters input sequencing reads to require at least one mate pair to contain RT DNA sequences. Next, Retrofind conducts an alignment on the pre-filtered reads using the BWA mem aligner under strict conditions (Li and Durbin 2009). Samtools coordinate sorts, and Picard tools remove duplicates from the alignment (Li *et al.* 2009). Reads inconsistent with a proper mate pairing or with larger than expected insert size are identified as a discordant read pair. Split reads were identified from reads aligning with soft or hard clipping above a threshold. Candidate split and discordant reads were aligned using BWA mem to a list of consensus sequences derived from Repbase (Bao *et al.* 2015). Candidate reads were then grouped into clusters using bedtools and designated as 5′ (left) and 3′ (right) junction reads (Quinlan and Hall 2010). Next, a heuristic process was applied to the left and right junction to identify a retrotransposition that satisfies filtering options. If there is at least one right junction and one left junction split read, a TSD prediction is made. There is an option to require a TSD prediction within a user-defined range. The default TSD size range we consider is 2–30 base pairs. The exported file includes an identification number that can be used to link reads of support to the transposition call. Last, Retrofind also outputs de novo assembly of supporting reads using the Megahit short read assembler (Li *et al.* 2015) and a BWA mem alignment of assembled contigs to the genome. The reads of support and assembled contig alignment can be visually inspected using a genome browser. Retrofind was validated using the pipeline and methods described in (Siudeja *et al.* 2021).

De novo TE insertions detected in both young and old IFM nuclei were compared to the bulk genomic DNA to exclude the insertions that are present within the germline. The genomic location of insertions identified in w^{1118} was determined using ChIPSeeker (Yu *et al.* 2015). High quality insertions were defined as insertions detected in both pipelines and validated visually using IGV.

Statistical analyses

All statistical analyses except for the RNA-sequencing data were performed using GraphPad Prism Version 9.5.1 (733). Statistics for the RNA-sequencing data are further detailed in the RNA-sequencing methods section. An unpaired t-test was used to compare the number of new insertions with age. An unpaired t-test with Bonferroni correction was used for qPCR analysis. Dunnett test was used for lifespan data and survival curves. A Gehan-Breslow-Wilcoxon test was used to compare median lifespans. A permutation test (95th percentile/top 5%) followed by a two-sided t-test with correction for multiple comparisons was used to compare maximum lifespan. A Chi-square test for trend was used to analyze the negative geotaxis data. A one-way ANOVA was used for thermal stress assays, fecundity, fertility, body weight, and bacterial infection assays.

Results

TE insertions do not increase with age

To identify de novo TE insertions, we whole genome sequenced 21 individual nuclei from young (day 5) and old (day 50) animals (Fig. 1a). Using this methodology, new insertions are represented in approximately half of the reads from each nucleus, facilitating robust detection. We carried out our studies using the well characterized w^{1118} strain that shows a typical lifespan and is often used as a wild-type control (Fig. 1a) (Qiu *et al.* 2017; Yang *et al.* 2022). We chose to focus on the thorax of flies, as this region of the fly has a higher mutation rate in comparison to the head or the abdomen based on a *LacZ* mutation reporter transgene (Garcia *et al.* 2010). Moreover, these mutations were mostly genomic rearrangements caused by the inaccurate repair of double stranded breaks that could be caused by TE activity (Garcia *et al.* 2010). To distinguish new insertions that occur with age from pre-existing ones within the germline genome, we defined the TE landscape in the w^{1118} strain by carrying out bulk sequencing from pooled thoraces from young flies to a total depth of 157× coverage. Sequencing data was analyzed using a newly developed in-house TE detection pipeline called Retrofind, in addition to a published pipeline that has successfully detected somatic insertions in clonally expanded tumors, so serves as independent validation (Siudeja *et al.* 2021). New TE insertions were identified by similar criteria for each pipeline by detecting both split and discordant reads of evidence from paired-end sequencing data. Additionally, newly called insertion sites in the germline genome needed to possess the TSD that occurs because of the double stranded break made by the TE-encoded integrase. A total of 871 TE insertions unique to w^{1118} relative to the *dm6* reference genome were detected by the two pipelines, with 505 being detected by both (Fig. 1b; Supplementary Table 3). We consider these to be high confidence insertions. TE insertions identified in w^{1118} were primarily within intronic and intergenic regions and were largely excluded from promoters (+/− 100 base pairs of the transcription start site) and coding sequences (CDS) where they might disrupt gene function (Fig. 1c).

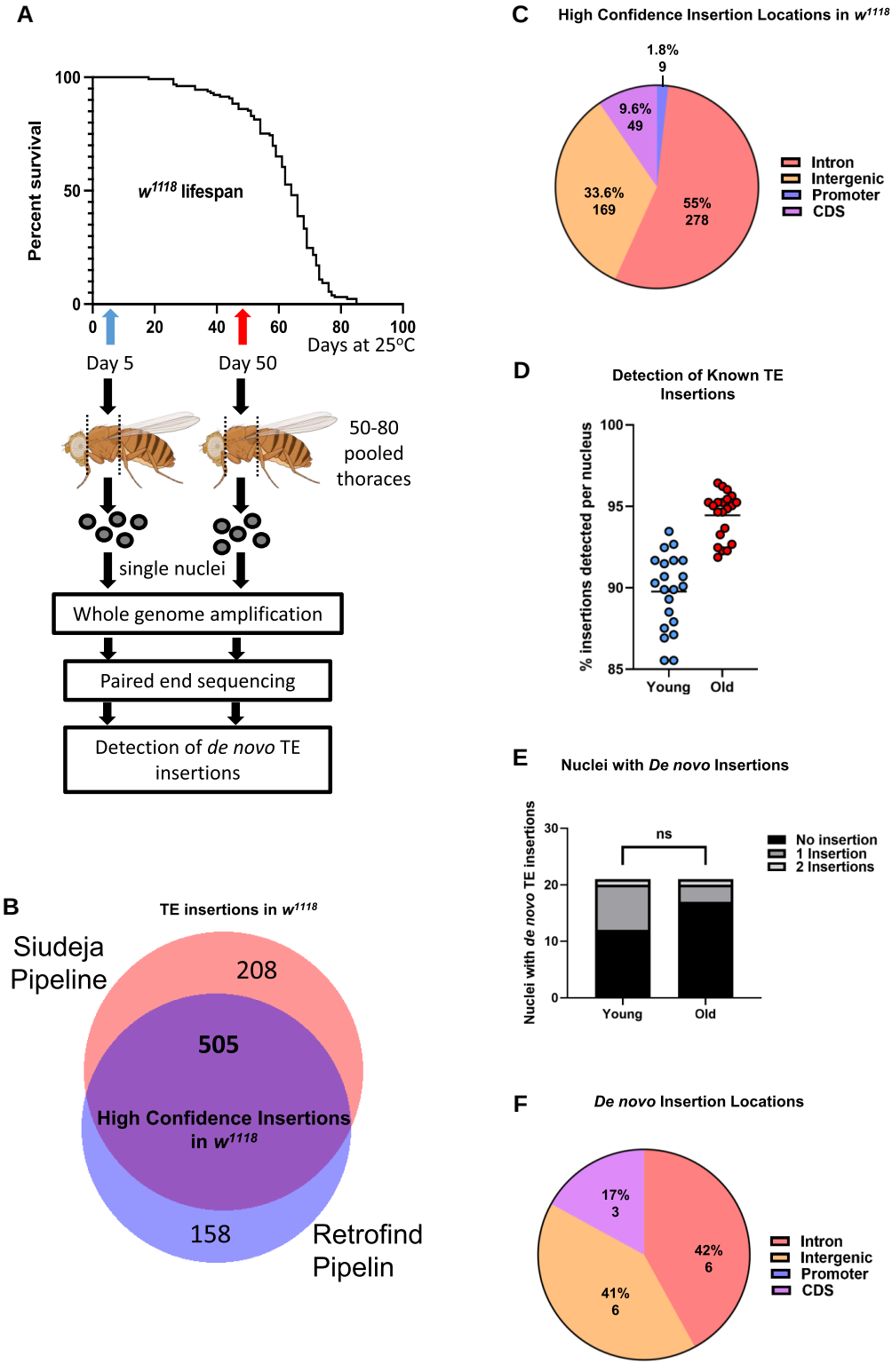

Fig. 1. Single cell WGS of young (day 5) and old (day 50) *Drosophila* thoraces. a) A schematic of the workflow of the isolation of single nuclei and how new TE insertions were detected. The typical w^{1118} wild type strain lifespan is also displayed. Flies in this image were created with BioRender.com b) The number of new TE insertions in the w^{1118} strain from the bulk WGS in comparison to the sequenced reference strain (dm6) using both the pipeline from Siudeja et al (Siudeja *et al.* 2021) and Retrofind. Five hundred five insertions were called by both pipelines, which we deem high confidence insertions. This was created using (Oliveros 2007–2015). c) The distribution of the genomic locations where the high confidence w^{1118} strain TE insertions fall. d) The number of known TE insertions (strain/background insertions) that were able to be detected within each nuclear sample represented as a percentage of the insertions detected in the sample out of total strain insertions. Each dot represents a nucleus. e) The number of nuclei with new TE insertions represented as a stacked bar graph comparing young and old samples. No new insertions (black), 1 new insertion (gray), 2 new insertions (light gray). New insertions are defined as insertions not previously called within the strain or other nuclei. Unpaired t-test. ns $P = 0.1809$. f) The distribution of genomic locations where the 15 new TE insertions within individual nuclei fall.

To determine if the number of TE insertions increased with age in somatic cells, we isolated and amplified genomic DNA from 21 individual nuclei from thoraces of young (5-day-old) and from old (50-day-old) flies (Fig. 1a). WGS of these 42 nuclei revealed an average 317× coverage of the genome for nuclei from young thoraces and 354× coverage for nuclei from old thoraces. To confirm our ability to map TEs in individual nuclei, we looked for the 505 high confidence TE insertions detected from sequencing bulk genomic DNA. Confirming a robust ability to detect TEs, we found an average of 90% of high-confidence insertions in nuclei from young animals and 94% from old animals (Fig. 1d). While it is notable that more of the known w^{1118} insertions were detected in nuclei from old animals, this likely reflects the higher sequencing depth observed with these samples.

To identify de novo insertions, we used Retrofind and the published pipeline to analyze the sequencing data for each nucleus, with unique insertions detected by both pipelines being deemed high confidence (Siudeja *et al.* 2021). This revealed that there was not a significant increase in insertions in nuclei from old animals when compared to young animals (Fig. 1e). Indeed, 57 and 76% of nuclei from young and old animals, respectively, did not have any new TE insertions, and a maximum of 2 insertions were detected in any individual nucleus. A total of 15 new insertions were found across 9 nuclei from young animals and 4 from old animals, which were visually confirmed using integrated genome viewer (IGV), similar to previous studies (Siudeja *et al.* 2021). Like existing TE insertions within the genome, new insertions occurred primarily in non-coding regions of the genome (Fig. 1f). Most of the new insertions observed in nuclei from young flies, and all the insertions observed in old flies, were the *hobo* element (also known as the *H-element*) (Supplementary Table 4). This DNA terminal inverted repeat transposon is an evolutionarily recent addition to the *Drosophila* genome that is known to be active (Periquet *et al.* 1994). In addition, the long terminal repeat (LTR) RT *HMS-Beagle* and the DNA *S terminal inverted repeat element* showed a new single insertion in the somatic genome, each in a single nucleus from young animals. To ensure that TEs had the potential for mobilization in tissues of the thorax, we tested the expression of a range of TEs in the w^{1118} flies. Using qPCR, we found that all TEs tested had detectable levels of mRNA in young and old flies and generally showed a small increase with age, similar to reports using other tissues such as the fat body (Supplementary Fig. 1) (Chen *et al.* 2016). Thus, despite being expressed throughout adulthood, TE expression does not lead to additional insertional events.

Because our single nuclei were isolated from thoraces, they likely represent several different cell types, possibly obscuring an increase in TEs that might be observed by analyzing a single tissue. We therefore also purified nuclei from IFMs, which are a major muscle group in the thorax that show age-associated decline (Josephson *et al.* 2000; Agianian *et al.* 2004; Demontis *et al.* 2014; Jawkar and Nongthomba 2020). To purify IFM nuclei, they were labeled by expressing a nuclear membrane localized GFP (UAS-GFP:KASH) using UH3-Gal4 (UH3 > GFP:KASH; Fig. 2a) (Singh *et al.* 2014). Individual GFP positive nuclei from dissected thoraces were isolated by FACS and whole genome amplified in a similar manner to our analyses of thoracic nuclei. Unamplified, bulk DNA from the abdomen and head regions of the same flies were sequenced to a total of 443× coverage to exclude strain-specific TE insertions. Sequencing of individual nuclei revealed an average of 64× coverage from young nuclei and 115× from old. Like our findings using nuclei from thoraces, analyses of 6 and 7 IFM nuclei from young and old flies, respectively, revealed no significant increase in TE insertions with age (Fig. 2b). Approximately half of nuclei examined had no new insertions and the small number that was observed were inserted into intergenic or intronic sequences (Fig. 2c). These data show that TE insertions do not increase significantly during aging in cells of the thorax or IFMs.

Reduced expression of individual RTs is associated with extended lifespan

While no increase in TE insertions were observed during adulthood, the expression of these elements could impact cell function, thereby altering lifespan. For this reason, we examined the effect of attenuating RT expression. We chose to focus initially on the RT *412*, which is part of the *gypsy* super-family of LTR elements. This element is stable in the germline, making it a good candidate for examining the effects of transposon expression (Supplementary Table 3) (Di Franco *et al.* 1992). Indeed, even in contexts where TEs are particularly active, such as the reduction of the RNAi pathway and in tumors, no new *412* insertions were detected (Siudeja *et al.* 2021; Yang *et al.* 2022). Like most RTs, *412* is multi-copy within the genome, having 36 copies in total, 24 of which are full length and present in euchromatin (Gramates *et al.* 2022). We therefore used a knockdown approach to reduce the expression of *412* to assess the effect on life- and healthspan. To do this, we generated two UAS-regulated short hairpin transgenes, 412#1, and 412#2, in addition to a control construct expressing a shRNA predicted not to target any mRNAs (control). Driving the expression of UAS-shRNA transgenes targeting *412* with the ubiquitous Actin5C-Gal4 (Act5C > shRNA) driver led to an ∼2-fold reduction in *412* mRNA levels (Fig. 3a). Importantly, this transgene is 412-specific, as expression other RTs were not significantly altered in these knockdown animals (Supplementary Fig. 2). *412* knockdown flies completed metamorphosis normally and were grossly morphology normal (Supplementary Fig. 3). Quantifying the lifespan of these animals revealed significantly extended median and maximum lifespan compared to controls (Fig. 3b–d).

To confirm the lifespan extension caused by RNAi-mediated knockdown of *412*, we additionally used CRISPRi to reduce expression of this TE. To do this, we generated a UAS transgene encoding an enzymatically dead Cas9 protein fused to the *KRAB* transcriptional repressor (UAS-dCas9:KRAB). dCas9:KRAB was targeted to the *412* LTR enhancer/promoter region using a transgene expressing a guide RNA (gRNA) under the control of the ubiquitously expressed, *U6* promoter (412gRNA). As a control, we generated a non-targeted gRNA (control gRNA). CRISPRi was carried out by crossing Act5C > dCas9:KRAB and 412gRNA flies, which led to a 1.7-fold reduction in 412 mRNA levels (Fig. 3e). In contrast to 412 knockdown adult flies that were indistinguishable from controls, 412gRNA CRISPRi flies were 7% heavier than control gRNA flies although they were morphologically normal (Supplementary Fig. 3). Mirroring our shRNA results, 412 gRNA-expressing flies showed extended median and maximum lifespan compared to control gRNA-expressing flies (Fig. 3f–h). Reducing the expression of a single RT is therefore sufficient to extend lifespan.

Utilizing the same control and 412 gRNA-expressing flies, we used CRISPRa to perform the converse experiment to assess whether overexpressing a single RT would shorten lifespan. This required combining the control and 412 gRNA transgenes with ubiquitous expression of a UAS transgene encoding an enzymatically dead Cas9 protein fused to a VPR transcriptional activator (Act5C > dCas9:VPR). Adult 412gRNA CRISPRa flies showed a 2.5-fold increase in 412 mRNA levels and were phenotypically indistinguishable from control gRNA CRISPRa flies (Fig. 3i;

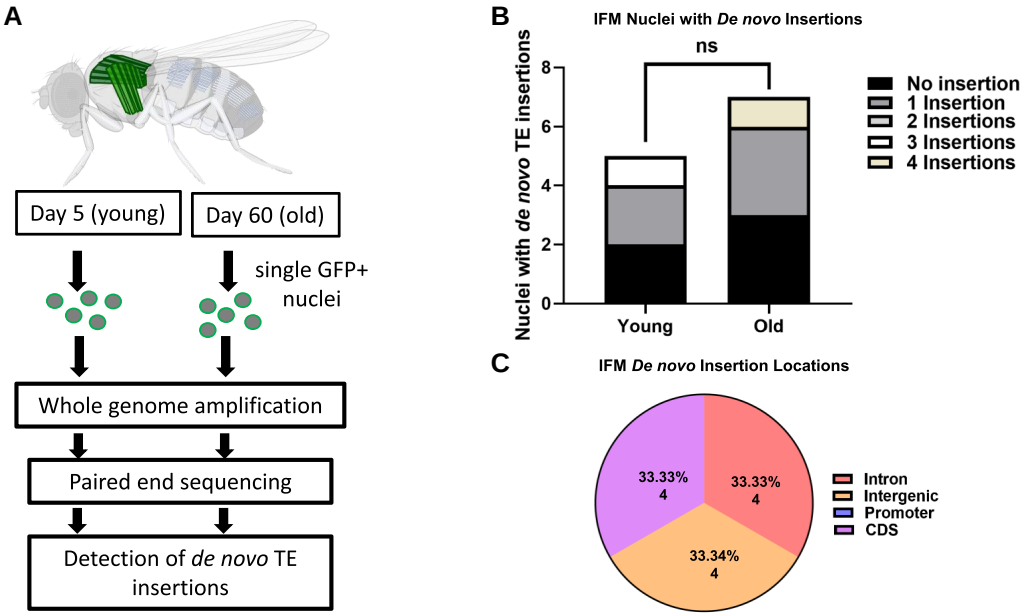

Fig. 2. Single cell WGS of young (day 5) and old (day 60) *Drosophila* IFMs. a) A schematic of the workflow of the isolation of single nuclei and how new TE insertions were detected from IFMs. Flies in this image were created with BioRender.com. b) The number of nuclei with new TE insertions represented as a stacked bar graph comparing young and old samples. No new insertions (black), 1 new insertion (gray), 2 new insertions (light gray), 3 new insertions (white), 4 new insertions (tan). New insertions are defined as insertions not previously called within the strain or other nuclei. Unpaired t-test. ns $P > 0.9999$. c) The distribution of genomic locations where the new TE insertions within individual IFM nuclei fall.

Supplementary Fig. 3). Contrasting our results seen using KRAB-mediated repression of *412*, activation of this TE led to decreased median and maximum lifespan compared to control gRNA flies (Fig. 3j–l). Thus, increasing the expression of a single RT is sufficient to attenuate lifespan.

To test whether changes in lifespan were specific to *412*, we reduced the expression of another RT, *Roo*, which showed 112 new insertions in w^{1118} compared to the annotated *Drosophila* genome (Supplementary Table 3). Driving the expression of a UAS-shRNA transgene targeting *Roo* using Act5C-Gal4 led to a ~2-fold reduction in mRNA levels and did not adversely affect ability of animals to complete metamorphosis or their gross morphology (Fig. 3m; Supplementary Fig. 3). Quantifying the lifespan of these animals revealed a significantly extended median and maximum lifespan compared to control animals (Fig. 3n–p). The expression of *412* and *Roo* therefore both contribute to aging.

Long-lived *412* or *Roo* knockdown flies do not show improved locomotion or stress resistance

Extension of longevity can be associated with improved healthspan, which can be measured as a delay in the onset of age-associated phenotypes. For example, long-lived fly strains, such as those with reduced insulin signaling, show increased resistance to starvation and oxidative stress (Broughton *et al.* 2005). Additionally, progeroid flies have an accelerated decline in locomotor activity with age (Cassidy *et al.* 2019). We therefore tested the extent to which flies with reduced expression of *412* or *Roo* showed improvements in locomotion and/or resistance to a range of stress conditions. One classic indicator of age-associated decline is reduced locomotion, which can be quantified using a negative geotaxis assay. As expected, locomotor ability declined with age across genotypes, with those in midlife (18 days old) and old age (40 days old) showing an attenuated negative geotaxis response compared to young flies (5 days old) (Supplementary Fig. 4). Midlife flies also have more locomotion when compared to old age flies (Supplementary Fig. 4). At all ages tested, *412* knockdown flies displayed locomotor capacity that was either indistinguishable (412#2) or worse (412#1) than control animals (Fig. 4a; Supplementary Fig. 4). Similarly, the locomotor capacity of *Roo* knockdown animals was not different from control animals (Fig. 4a).

To assess whether reduced RT expression altered resistance to oxidative stress, we treated ubiquitous *412* or *Roo* knock down flies with paraquat and quantified survival compared to control flies. This revealed that the two *412* shRNA transgenes behaved differently from each other, with 412#2 showing no change to survival and 412#1 having slightly reduced resistance to oxidative stress (Fig. 4b). *Roo* knockdown animals showed no change in resistance to oxidative stress compared to control animals (Fig. 4b). We additionally tested survival in response to: endoplasmic reticulum (ER) stress through treatment with the antibiotic tunicamycin (Chow *et al.* 2013), starvation, and thermal stress (cold and heat). None of these treatments led to a consistent change in survival for *412* or *Roo* knockdown flies, except starvation, where both *412* knockdowns showed increased sensitivity (Fig. 4c–f). An additional corollary to increased lifespan is a decline in fertility (Jasienska *et al.* 2006). We therefore quantified fecundity of *412* and *Roo* knockdown flies by counting the number of eggs laid per day and found no significant difference (Fig. 4g). Nor was the fertility of *412* or *Roo* knockdown animals altered, as the number of adult flies produced from those eggs was indistinguishable from controls (Fig. 4h). Combined, these assays show that reducing *412* or *Roo* expression does not improve standard assays of health and/or stress resistance that might be expected in these long-lived flies.

TE knockdown affects the expression of genes linked to proteolysis and immunity

To gain insight into the cellular changes caused by reduced TE expression, we performed RNA-seq on thoraces of Act > shRNA animals at mid-life (day 20). We chose mid-life as others have seen

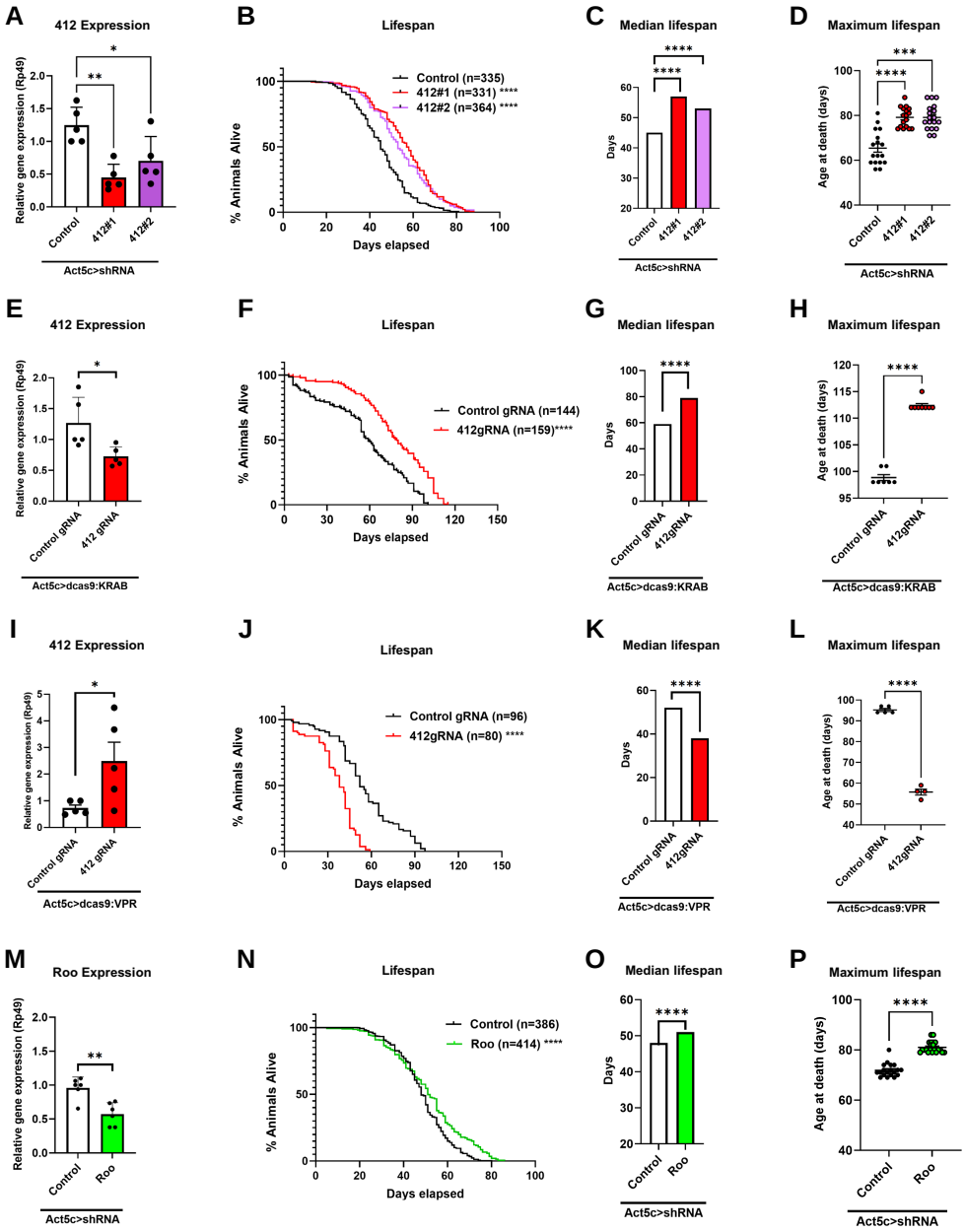

Fig. 3. Lifespan of ubiquitous shRNA and CRISPRi knockdown and CRISPRa overexpression of the retrotransposons, *412* and *Roo*. a) qPCR using SYBR green showing levels of *412* mRNA relative to *Rp49* (*Rpl32*) from adult flies expressing a control shRNA transgene under the control of Act5C-Gal4 compared to the *412* shRNA knockdowns (Act5C > shRNA). The experiment was performed in five biological replicates. An unpaired t-test with Bonferroni correction was used. (412#1) $^{**}P = 0.0018$. (412#2) $^{*}P = 0.0219$. b) Survival of the *412* shRNA lines compared to control shRNA driven ubiquitously by Act5C (Act > shRNA). Dunnett test. $^{****}P < 0.0001$. c) Median lifespan of the *412* shRNAs compared to control shRNA driven ubiquitously by Act5C (Act > shRNA). Gehan–Breslow–Wilcoxon test. $^{****}P < 0.0001$. d) Maximum lifespan of the *412* shRNAs compared to control shRNA driven ubiquitously by Act5C (Act > shRNA). Permutation test (95th percentile/top 5%) followed by two-sided t-test with correction for multiple comparisons. (412#1) $^{****}P < 0.0001$. (412#2) $^{***}P = 0.0001$. e) qPCR using SYBR green of 412gRNA CRISPRi compared to the control gRNA control (Act5C > dcas9-KRAB) relative to *Rp49* (*Rpl32*). The experiment was performed in five biological replicates. An unpaired t-test with Bonferroni correction was used. $^{*}P = 0.0269$. f) Survival of the CRISPRi driven ubiquitously by Act5C (Act > dcas9KRAB) with the 412gRNA compared to control gRNA. Dunnett test. $^{****}P < 0.0001$. g) Median lifespan of the CRISPRi driven ubiquitously by Act5C (Act > dcas9KRAB) with the 412gRNA compared to control gRNA. Gehan–Breslow–Wilcoxon test. $^{****}P < 0.0001$. h) Maximum lifespan of the CRISPRi driven ubiquitously by Act5C (Act > dcas9KRAB) with the 412gRNA compared to control gRNA. Permutation test (95th percentile) followed by two-sided t-test with correction for multiple comparisons. $^{****}P < 0.0001$. i) qPCR using SYBR green of 412gRNA CRISPRa compared to the control gRNA control (Act5C > dcas9-VPR) relative to *Rp49* (*Rpl32*). The experiment was performed in five biological replicates. An unpaired t-test with Bonferroni correction was used. $^{*}P = 0.0400$. j) Survival of the CRISPRa driven ubiquitously by Act5C (Act > dcas9VPR) with the 412gRNA compared to control gRNA. Dunnett test. $^{****}P < 0.0001$. k) Median lifespan of the CRISPRa driven ubiquitously by Act5C (Act > dcas9VPR) with the 412gRNA compared to control gRNA. Gehan–Breslow–Wilcoxon test. $^{****}P < 0.0001$. l) Maximum lifespan of the CRISPRa driven ubiquitously by Act5C (Act > dcas9VPR) with the 412gRNA compared to control gRNA. Permutation test (95th percentile) followed by two-sided t-test with correction for multiple comparisons. $^{****}P < 0.0001$. m) qPcR using SYBR green of the *Roo* mRNA KD compared to the control shRNA control (Act5C > shRNA) relative to *Rp49* (*Rpl32*). The experiment was performed in six biological replicates. An unpaired t-test with Bonferroni correction was used. $^{**}P = 0.0022$. n) Survival of the *Roo* shRNA compared to control shRNA driven ubiquitously by Act5C (Act > shRNA). Dunnett test. $^{****}P < 0.0001$ o) Median lifespan of the *Roo* shRNA compared to control shRNA driven ubiquitously by Act5C (Act > shRNA). Gehan–Breslow–Wilcoxon test. $^{****}P < 0.0001$. p) Maximum lifespan of the *Roo* shRNA compared to control shRNA driven ubiquitously by Act5C (Act > shRNA). Permutation test (95th percentile) followed by two-sided t-test with correction for multiple comparisons. $^{****}P < 0.0001$.

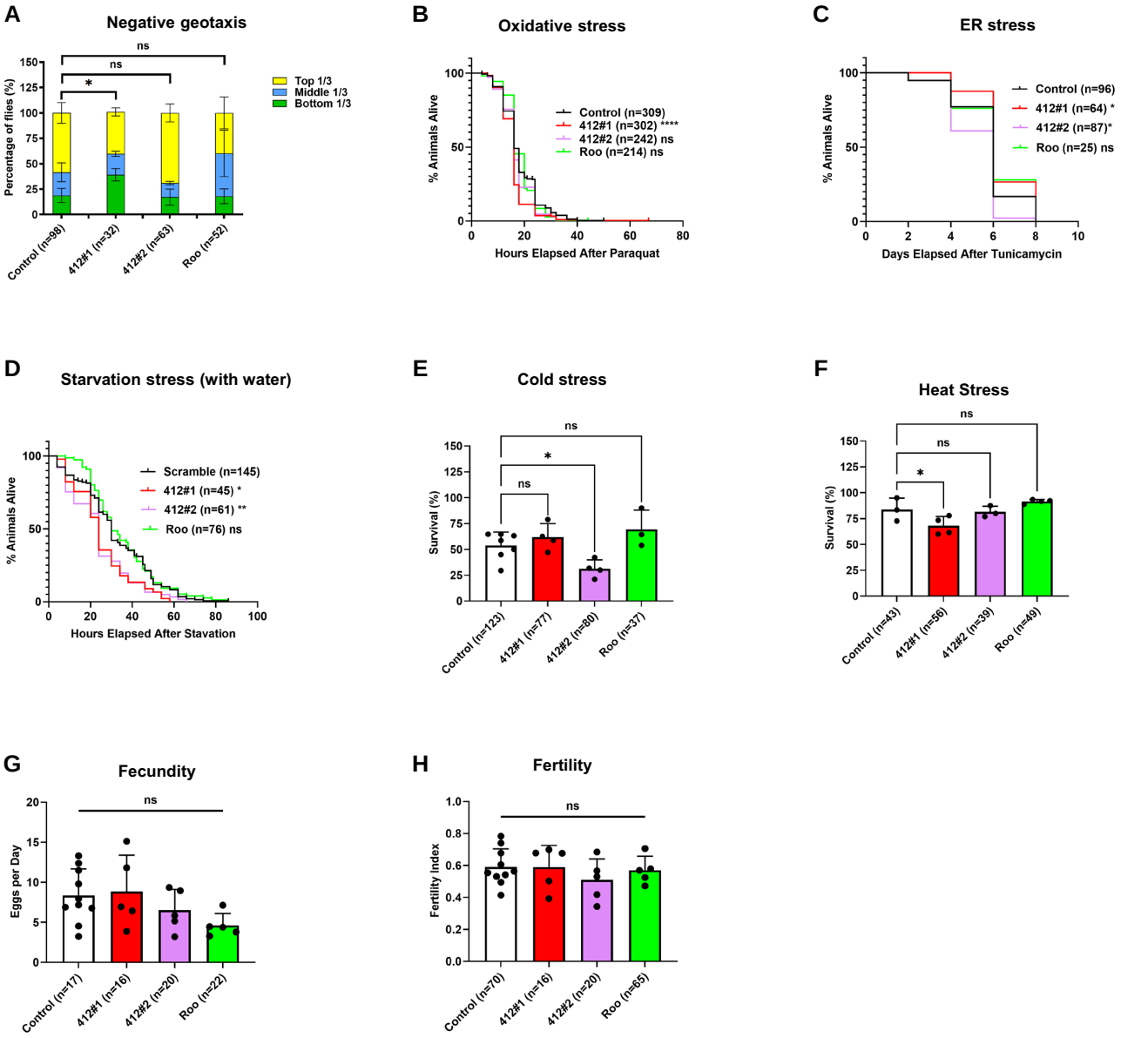

Fig. 4. Stress resistance assays of *412* and *roo* knockdown animals. a) Act5c > shRNA day 18 measurement of locomotion via negative geotaxis assay. The percentages of flies in each third of the vial are displayed. Chi-square test for trend. *(412#1) $P = 0.0428$. ns (412#2) $P = 0.1434$. ns (Roo) $P = 0.1934$. b) Act5c > shRNA day 40 response to oxidative stress by feeding paraquat and measuring survival. Dunnett test. ****(412#1) $P < 0.0001$. ns (412#2) $P = 0.0702$. ns (Roo) $P > 0.9999$. c) Act5c > shRNA day 20 response to endoplasmic reticulum (ER) stress by feeding tunicamycin and measuring survival. Dunnett test. *(412#1) $P = 0.0451$. *(412#2) $P = 0.0401$. ns (Roo) $P = 0.6156$. d) Act5c > shRNA day 40 response to starvation by only giving the flies access to water and measuring survival. Dunnett test. *(412#1) $P = 0.0298$. **(412#2) $P = 0.0037$. ns (Roo) $P = 0.4790$. e) Act5c > shRNA day 20 response to cold stress by keeping flies at 4 degrees Celsius and measuring survival after 48-hours recovery. Each dot is a vial or replicate of approximately 20 flies. One-way ANOVA. ns (412#1) $P = 0.0703$. * (412#2) $P = 0.0461$. ns (Roo) $P = 0.6592$. f) Act5c > shRNA day 20 response to heat stress by keeping flies at 37 degrees Celsius and measuring survival after 48-hours recovery. Each dot is a replicate of approximately 20 flies. One-way ANOVA. * (412#1) $P = 0.0498$. ns (412#2) $P = 0.9645$. ns (Roo) $P = 0.3978$. g) Act5c > shRNA day 25 measurement of fecundity. Data is displayed as average number of eggs laid per day over 5 days. Each dot represents a day for the number of flies in one vial. One-way ANOVA. ns (412#1) $P = 0.9925$. ns (412#2) $P = 0.7231$. ns (Roo) $P = 0.1803$. h) Act5c > shRNA day 25 measurement of fertility. Fertility index is calculated as number of progeny divided by number of eggs laid. Data is displayed as an average fertility index over 5 days. Each dot represents a day for the number of flies listed. One-way ANOVA. ns (412#1) $P > 0.9999$. ns (412#2) $P = 0.5881$. ns (Roo) $P = 0.9887$.

changes to age-associated phenotypes at this time point (Li *et al.* 2013; Cassidy *et al.* 2019). 332 differentially expressed genes (DEGs) were identified in 412 knockdown animals compared to control shRNA expressing flies using a 5% false discovery rate (FDR) cutoff. 212 of these genes were upregulated while 120 were downregulated and averaged a log2 fold change of 2.5 and 1.5, respectively (Fig. 5a; Supplementary Table 5). Functional analyses of upregulated genes using GO DAVID revealed significant enrichment in the single GO category of proteolysis using a 1% FDR (Huang da *et al.* 2009; Sherman *et al.* 2022). Many of these genes were members of the Jonah (Jon) family of serine proteases, including *Jonah 25Bi-iii*, *Jonah 44E*, *Jonah 65Aiii*, *Jonah 65Aiv*, *Jonah 74E*, and *Jonah 99Ci-iii* (Supplementary Table 7) (Huang da *et al.* 2009; Sherman *et al.* 2022). Similar GO analyses of downregulated genes did not reveal any significantly enriched categories.

To determine the extent to which knockdown of *Roo* led to similar changes to gene expression as *412*, we carried out RNA-seq analyses using thoraces of ubiquitous *Roo* knockdown flies. 344 genes

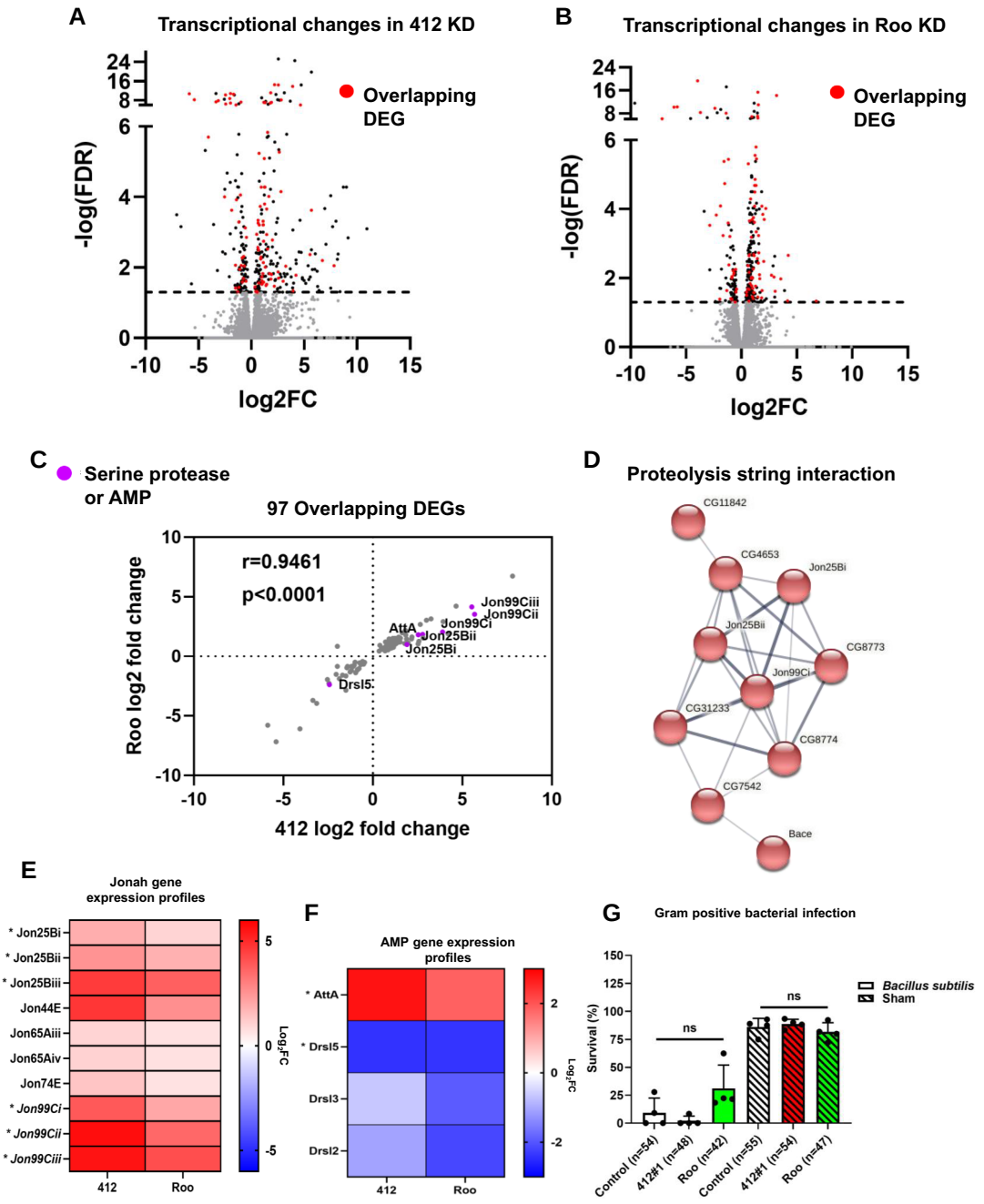

Fig. 5. Transcriptomic analysis of *412* and *Roo* knockdown animals. a) Volcano plot of DEGs from whole thorax of Act5c > 412#1 shRNA knockdown animals compared to control shRNA animals. Genes with a FDR < 0.05 are highlighted in black and above the dashed line. Genes that are differentially expressed in both *412* and *Roo* knockdown animals (overlapping genes) are highlighted in red. b) Volcano plot of DEGs from whole thorax of Act5c > Roo shRNA knockdown animals compared to control shRNA animals. Genes with a FDR < 0.05 are highlighted in black and above the dashed line. Genes that are differentially expressed in both *412* and *Roo* knockdown animals (overlapping genes) are highlighted in red. c) Correlation of Log_2FoldChange (Log2FC) of the overlapping DEGs between *412* and *Roo* knockdown animals. r = 0.9461. Deming regression. $P < 0.0001$. Serine proteases and AMPs that are also DEGS are enlarged and highlighted in purple. d) Gene interaction clustering performed on the overlapping DEGs using String with single nodes removed and 1 cluster used. There is a serine protease cluster of genes interacting. e) Heatmap of log2fold change (Log2FC) from RNA-Seq data across samples of the *Jonah* (*Jon*) genes. The * marked genes are significantly differentially expressed in both *412* and *Roo* knockdown thoraces. All other genes are significantly differentially expressed in just *412* knockdown thoraces. f) Heatmap of log2fold change (Log2FC) across samples of the AMPs. The * marked genes are significantly differentially expressed in both *412* and *Roo* knockdown thoraces. All other genes are significantly differentially expressed in just *412* knockdown thoraces. g) Act5c > shRNA day 20 response to gram positive bacterial infection (*Bacillus subtils*) and sham infection (PBS) measuring survival after 48-hours. Each dot is a replicate of approximately 20 flies. One-way ANOVA bacterial infection. ns (412) $P = 0.7186$. ns (Roo) $P = 0.1074$. One-way ANOVA sham infection. ns (412) $P = 0.8145$. ns (Roo) $P = 0.5828$. Unpaired t-test bacterial vs sham infection. ****(Control) $P < 0.0001$ ****(412) $P < 0.0001$. **(Roo) $P = 0.0042$.

were found to be differentially expressed in *Roo* knockdown animals, 236 of which were upregulated average and 108 were down compared to control animals (5% FDR; Fig. 5b; Supplementary Table 6). As with knockdown of *412*, the changes to gene expression in response to reduced *Roo* expression were relatively small, averaging 1.1 and 1.3 log2 fold change for up- and downregulated genes,

respectively. Interestingly, upregulated genes were enriched for the same proteolysis GO term as was observed in *412* knockdown animals (Huang da *et al.* 2009; Sherman *et al.* 2022) (1% FDR cutoff; Supplementary Table 8). No GO terms were significantly enriched among the downregulated genes.

Based on the identification of the same GO term in *412* and *Roo* knockdown datasets, we compared the transcriptional changes of these two strains. This revealed 97 genes common to both datasets, a majority of which behaved similarly ($r = 0.9461$; $P < 0.0001$; Fig. 5c). These genes were enriched for the single GO term of proteolysis (Huang da *et al.* 2009; Sherman *et al.* 2022) (1% FDR cutoff; Supplementary Table 9). To understand the relationship between genes observed to be dysregulated within the proteolysis GO category, we used STRING, which revealed a distinct interaction node mainly based on co-expression and co-occurrence (Fig. 5d) (Szklarczyk *et al.* 2021). The *Jon* genes, a family of serine proteases, were at the center of this node (Miguel-Aliaga *et al.* 2018). Two thirds of the genes affected by *412* and *Roo* knockdown were upregulated in knockdown flies, including all the genes within the proteolysis category (Fig. 5e). While little is known about the Jonah proteins, their expression appears to be primarily in the gut, where they are assumed to aid in digestion (Miguel-Aliaga *et al.* 2018). However, expression of the *Jon* genes has also been linked with changes in the immune deficient (IMD) and Toll immunity pathways, which have previously been associated with lifespan regulation (Akam and Carlson 1985; Carpenter *et al.* 2009; Yadav and Eleftherianos 2019). When the GO category FDR was expanded to 5%, the term "negative regulation of melanin biosynthetic process" was also present indicating a potential role in the immune system (Huang da *et al.* 2009; Sherman *et al.* 2022) (Supplementary Table 9). Consistent with this, the expression of AMPs that are downstream of the IMD and Toll pathways were affected in *412* or *Roo* knockdown flies, with several *Drosomycins* (e.g. *Drsl2*, *Drsl3*, *Drsl5*) significantly downregulated and *Attacin-A* (*AttA*) being significantly upregulated (Fig. 5f). These data suggest that TEs such as *412* and *Roo* alter the expression of genes related to proteolysis regulation and the immune system to influence longevity. The changes to the expression of the immune *Drosomycin* genes were relatively modest, suggesting a chronic, low level, change to immune function. This may, however, lead to an altered response to acute bacterial infection in TE knockdown flies. To test this, we infected flies with *Bacillus subtilis*, a Gram-positive bacteria that activates the Toll pathway. Infecting flies by direct bacterial injection of thoraces led to a dramatic increase in lethality 48 hours post infection compared to sham-injected controls (Fig. 5g). However, there was no difference in survival between TE knockdown and control flies (Fig. 5g). Thus, the downregulation of *Drosomycins* does not lead to a change in survival in response to acute bacterial infection.

Discussion

In this study we find that there is no significant increase in TE mobilization with age in *Drosophila*, indicating that they have a robust mechanism for preventing de novo TE insertions in somatic cells. Based on the observation that reduced activity of the RNAi pathway leads to an increase in TE insertions with age, this mechanism is likely a key means of limiting de novo TE insertions during normal aging (Yang *et al.* 2022). By combining a single nucleus WGS approach with analyses using two pipelines, we are confident that new insertions would have been detected if present. Prior to our study, the most compelling data indicating increased TE insertions with age in wild-type animals came from use of a TE reporter transgene and sequencing of bulk DNA samples (Siudeja *et al.* 2021; Ward *et al.* 2022; Yang *et al.* 2022). Use of a fluorescent reporter for the RT *mdg4* revealed age-associated de novo insertions in cells of the adult brain and fat body, although the frequency was low (Wood *et al.* 2016; Chang *et al.* 2019). In addition, examining the insertional proficiency of all TEs through long-read sequencing of pooled adult brains or midguts showed new insertions by several different elements, including *mdg4* and *Roo* (Siudeja *et al.* 2021). Like the *mdg4* reporter data, the number of new insertions detected using this approach was low, averaging less than one new integration event per individual (Siudeja *et al.* 2021). Because both approaches identified new insertions, it is possible that TEs are more highly expressed in the gut and brain than cells of the thorax, allowing some insertions to occur during aging in these tissues. Alternatively, given the low frequency of new TE insertions that were observed, it is more likely that these published data are congruent with our study. Based on the rate of transposition observed, our sequencing analyses of 42 thoracic nuclei (21 from young flies and 21 from old) was unlikely to be sufficient to detect new insertions. Consistent with our data that endogenous expression of TEs does not necessary lead to new insertions, overexpression of *mdg4* does not increase the number of genomic copies of this element (Rigal *et al.* 2022). We therefore suggest that new TE insertions are unlikely to be a key driver of cell and tissue dysfunction that occurs during normal aging. Interestingly, this contrasts with disorders such as cancer where there is clear evidence from mammalian cells and flies that TE insertions are a frequent occurrence that likely impact disease severity (Hancks and Kazazian 2016; Scott *et al.* 2016; Cajuso *et al.* 2019; Siudeja *et al.* 2021).

Previous functional evidence supporting TE mobilization playing a role in aging has come from the pharmaceutical approach of using RT inhibitors, with phosphonoformic acid (PFA), dideoxyinosine (ddI) in *Drosophila*, and Lamivudine (3TC), Stavudine (d4T) treatment in mice extending lifespan. (Driver and Vogrig 1994; Simon *et al.* 2019). NRTIs are well-established to block RT replication, thereby preventing RT reinsertion (Simon *et al.* 2019). However, RT inhibitor treatment can additionally decrease RNA levels of the *L1* element in human cells, thus the effect of these drugs may not be limited to restricting mobilization (Ward *et al.* 2022). If NRTIs exert similar effects in flies, the extended lifespan seen using these drugs could be due to reduced expression of some or all TEs, rather than changes to replicative capacity. This data, like ours showing that TE knockdown affects lifespan without increasing mobilization, suggests that the presence of TE mRNA may be detrimental to cell and animal function.

Because of their similarity to retroviruses, cytosolic DNA intermediates produced by RTs can trigger the activity of the immune system (Martin *et al.* 2018; De Cecco *et al.* 2019; Simon *et al.* 2019; Miller *et al.* 2021). In human cells, *L1* RT expression induces the interferon beta (*IFNβ*) inflammatory response (De Cecco *et al.* 2019; Miller *et al.* 2021). This can lead to chronic inflammation (inflammaging), which is common in aged individuals and is associated with cellular senescence (Miller *et al.* 2021). In mammals, recognition of cytosolic RT DNA by *Cyclic GMP-AMP synthase/Stimulator of interferon genes* (*cGAS/STING*) triggers the *Nuclear Factor Kappa B* (*NFκB*) pathway and the *IFNβ* inflammatory response (Martin *et al.* 2018; Simon *et al.* 2019). *Drosophila* does not have adaptive immunity, but many proteins that comprise the innate immune response are homologous to those that regulate the mammalian inflammatory response (Martin *et al.* 2018). In *Drosophila,* STING activates the *NFκB* homolog *Relish* (*Rel*) to activate the IMD pathway and the expression of AMPs (Martin *et al.*

2018). This functions in parallel to the Toll pathway that acts through *Dorsal-related immunity factor* (*Dif*), another *NFκB* homolog, to activate the production of AMPs (Valanne *et al.* 2011; Myllymäki *et al.* 2014; Khor and Cai 2020). We did not find altered expression of components of the upstream components of the IMD and Toll pathways in *412* or *Roo* knockdown animals. However, several *Drosomycin* genes that encode AMPs downstream of the Toll pathway activation were downregulated upon TE knockdown. Lowering the expression of AMPs extends lifespan (Lin *et al.* 2018), suggesting that this may contribute to the lifespan changes seen in TE knockdown flies. While the mechanism by which *412* or *Roo* knockdown alters the expression of AMP genes remains to be determined, it may be linked to the upregulation of genes involved in proteolysis. In particular, genes of the *Jonah* serine hydrolase family are activated upon RNA viral infection and can influence the expression of *Drosomycins*, although the mechanism for this is unknown (Carpenter *et al.* 2009; Yadav and Eleftherianos 2019). Jon proteins have a conserved function across species as their mammalian homolog, *Chymotrypsin like* (*CTRL*), is also involved in proteolysis within the gut (Hu *et al.* 2011; Parekh *et al.* 2011; Hu *et al.* 2017; Miguel-Aliaga *et al.* 2018; Hu *et al.* 2020). Recently, a chymotrypsin-trypsin fusion protease has been utilized as a treatment for inflammation and to promote wound healing, suggesting a conserved link between these serine proteases and inflammation (Shah and Mital 2018). Our TE knockdown flies did not show a difference in survival when challenged with an acute bacterial infection. We therefore hypothesize that the upregulation of the *Jonah* genes could dampen the immune system to decrease inflammation, and this could contribute to the extension of lifespan seen in animals with reduced TE expression. Given the similar results we obtained with *412* and *Roo*, this effect could be a general TE effect and similar results would be observed for a range of different TEs, although this remains to be tested.

Increased lifespan often coincides with improved stress resistance or other markers of health as illustrated by the insulin mutant and progeroid flies showing changes to oxidative stress and starvation and locomotion, respectively (Broughton *et al.* 2005; Cassidy *et al.* 2019). In contrast, knockdown of *412* or *Roo* increased lifespan without promoting observable stress resistance or delaying the onset of age-associated changes such as decreased mobility. Previous studies in *Drosophila* examining changes to heterochromatic and RNAi pathways to modulate TE activity did not examine these classic stress assays (Chen *et al.* 2016; Wood *et al.* 2016). Thus, it is possible that TE expression-induced changes to lifespan occur without altering stress resistance, effectively uncoupling life- and healthspan. Defining the precise links between *412*, *Roo* and other TEs and their effect on cellular and organism function during aging will require additional genetic and molecular studies to elucidate the links between the *Jonah* genes, immunity, and aging.

Data availability

RNA-seq data can be accessed through GEO Series accession number GSE207160. The thoracic WGS data can be accessed through the Sequence Read Archive (SRA) and are accessible through BioProject accession number: PRJNA854389. The indirect flight muscle WGS data can be accessed through the SRA BioProject accession number: PRJNA854818.

Supplemental material is available at GENETICS online.

Acknowledgements

We thank members of the Secombe, Vijg, and Baker labs for their insights throughout this project, particularly Shannon Lightcap who generated several transgenes used in this study, and Matanel Yheskel who helped with bioinformatic analyses. We are also very grateful to Alison Bardin and lab members for assistance with their TE insertion pipeline and Masako Suzuki, Jack Lenz, and Kenny Ye for their genomics and genetics expertise. We are grateful for fly strains from the Bloomington *Drosophila* Stock Center (NIH P400D018537).

Funding

This work was supported by National Institutes of Health R01 AG053269 to J.S., T32AG023475 and T32GM007491 to B.K.S, AG017242 and AG047200 to J.V., the shared instrument grant 1S10OD023591-01, and the Einstein Cancer Center Support Grant P30 CA013330.

Conflicts of interest

J.V. is a co-founder of Singulomics Inc., and MutaGentech Inc. The other authors declare no conflict of interest.

Literature cited

Agianian B, Krzic U, Qiu F, Linke WA, Leonard K, Bullard B. A troponin switch that regulates muscle contraction by stretch instead of calcium. EMBO J. 2004;23(4):772–779. doi:10.1038/sj.emboj.7600097.

Akam ME, Carlson JR. The detection of jonah gene transcripts in Drosophila by in situ hybridization. EMBO J. 1985;4(1):155–161. doi:10.1002/j.1460-2075.1985.tb02330.x.

Akbari OS, Bellen HJ, Bier E, Bullock SL, Burt A, Church GM, Cook KR, Duchek P, Edwards OR, Esvelt KM, *et al.* Biosafety. Safeguarding gene drive experiments in the laboratory. Science. 2015;349-(6251):927–929. doi:10.1126/science.aac7932.

Bao W, Kojima KK, Kohany O. Repbase update, a database of repetitive elements in eukaryotic genomes. Mob DNA. 2015;6(1):11. doi:10.1186/s13100-015-0041-9.

Broughton SJ, Piper MD, Ikeya T, Bass TM, Jacobson J, Driege Y, Martinez P, Hafen E, Withers DJ, Leevers SJ, *et al.* Longer lifespan, altered metabolism, and stress resistance in Drosophila from ablation of cells making insulin-like ligands. Proc Natl Acad Sci U S A. 2005;102(8):3105–3110. doi:10.1073/pnas.0405775102.

Cajuso T, Sulo P, Tanskanen T, Katainen R, Taira A, Hänninen UA, Kondelin J, Forsström L, Välimäki N, Aavikko M, *et al.* Retrotransposon insertions can initiate colorectal cancer and are associated with poor survival. Nat Commun. 2019;10(1):4022. doi:10.1038/s41467-019-11770-0.

Carpenter J, Hutter S, Baines JF, Roller J, Saminadin-Peter SS, Parsch J, Jiggins FM. The transcriptional response of Drosophila melanogaster to infection with the sigma virus (Rhabdoviridae). PLoS One. 2009;4(8):e6838. doi:10.1371/journal.pone.0006838.

Cassidy D, Epiney DG, Salameh C, Zhou LT, Salomon RN, Schirmer AE, McVey M, Bolterstein E. Evidence for premature aging in a Drosophila model of Werner syndrome. Exp Gerontol. 2019;127:110733. doi:10.1016/j.exger.2019.110733.

Chang YH, Keegan RM, Prazak L, Dubnau J. Cellular labeling of endogenous retrovirus replication (clevr) reveals de novo insertions of the gypsy retrotransposable element in cell culture and in both neurons and glial cells of aging fruit flies. PLoS Biol. 2019;17(5):e3000278. doi:10.1371/journal.pbio.3000278.

Chatterjee A, Roy D, Patnaik E, Nongthomba U. Muscles provide protection during microbial infection by activating innate immune

response pathways in Drosophila and zebrafish. Dis Model Mech. 2016;9(6):697–705. doi:10.1242/dmm.022665.

Chen H, Zheng X, Xiao D, Zheng Y. Age-associated de-repression of retrotransposons in the Drosophila fat body, its potential cause and consequence. Aging Cell. 2016;15(3):542–552. doi:10.1111/acel.12465.

Chow CY, Wolfner MF, Clark AG. Using natural variation in Drosophila to discover previously unknown endoplasmic reticulum stress genes. Proc Natl Acad Sci U S A. 2013;110(22):9013–9018. doi:10.1073/pnas.1307125110.

Corces MR, Trevino AE, Hamilton EG, Greenside PG, Sinnott-Armstrong NA, Vesuna S, Satpathy AT, Rubin AJ, Montine KS, Wu B, *et al.* An improved atac-seq protocol reduces background and enables interrogation of frozen tissues. Nat Methods. 2017;14(10):959–962. doi:10.1038/nmeth.4396.

Czech B, Malone CD, Zhou R, Stark A, Schlingeheyde C, Dus M, Perrimon N, Kellis M, Wohlschlegel JA, Sachidanandam R, *et al.* An endogenous small interfering RNA pathway in Drosophila. Nature. 2008;453(7196):798–802. doi:10.1038/nature07007.

De Cecco M, Criscione SW, Peckham EJ, Hillenmeyer S, Hamm EA, Manivannan J, Peterson AL, Kreiling JA, Neretti N, Sedivy JM. Genomes of replicatively senescent cells undergo global epigenetic changes leading to gene silencing and activation of transposable elements. Aging Cell. 2013;12(2):247–256. doi:10.1111/acel.12047.

De Cecco M, Ito T, Petrashen AP, Elias AE, Skvir NJ, Criscione SW, Caligiana A, Brocculi G, Adney EM, Boeke JD, *et al.* L1 drives ifn in senescent cells and promotes age-associated inflammation. Nature. 2019;566(7742):73–78. doi:10.1038/s41586-018-0784-9.

Demontis F, Patel VK, Swindell WR, Perrimon N. Intertissue control of the nucleolus via a myokine-dependent longevity pathway. Cell Rep. 2014;7(5):1481–1494. doi:10.1016/j.celrep.2014.05.001.

Di Franco C, Galuppi D, Junakovic N. Genomic distribution of transposable elements among individuals of an inbred Drosophila line. Genetica. 1992;86(1–3):1–11. doi:10.1007/BF00133706.

Dong X, Milholland B, Vijg J. Evidence for a limit to human lifespan. Nature. 2016;538(7624):257–259. doi:10.1038/nature19793.

Dong X, Zhang L, Milholland B, Lee M, Maslov AY, Wang T, Vijg J. Accurate identification of single-nucleotide variants in whole-genome-amplified single cells. Nat Methods. 2017;14(5):491–493. doi:10.1038/nmeth.4227.

Drelon C, Rogers MF, Belalcazar HM, Secombe J. The histone demethylase KDM5 controls developmental timing in Drosophila by promoting prothoracic gland endocycles. Development. 2019;146(24):24. doi:10.1242/dev.182568.

Driver CJ, Vogrig DJ. Apparent retardation of aging in Drosophila melanogaster by inhibitors of reverse transcriptase. Ann N Y Acad Sci. 1994;717(1):189–197. doi:10.1111/j.1749-6632.1994.tb12087.x.

Dufourt J, Dennis C, Boivin A, Gueguen N, Théron E, Goriaux C, Pouchin P, Ronsseray S, Brasset E, Vaury C. Spatio-temporal requirements for transposable element pirna-mediated silencing during Drosophila oogenesis. Nucleic Acids Res. 2014;42(4):2512–2524. doi:10.1093/nar/gkt1184.

Edgar R, Domrachev M, Lash AE. Gene expression omnibus: NCBI gene expression and hybridization array data repository. Nucleic Acids Res. 2002;30(1):207–210. doi:10.1093/nar/30.1.207.

Garcia AM, Calder RB, Dollé ME, Lundell M, Kapahi P, Vijg J. Age- and temperature-dependent somatic mutation accumulation in *Drosophila melanogaster*. PLoS Genet. 2010;6(5):e1000950. doi:10.1371/journal.pgen.1000950.

Ghildiyal M, Seitz H, Horwich MD, Li C, Du T, Lee S, Xu J, Kittler EL, Zapp ML, Weng Z, *et al.* Endogenous siRNAs derived from transposons and mRNAs in Drosophila somatic cells. Science. 2008;320(5879):1077–1081. doi:10.1126/science.1157396.

Gorbunova V, Boeke JD, Helfand SL, Sedivy JM. Human genomics. Sleeping dogs of the genome. Science. 2014;346(6214):1187–1188. doi:10.1126/science.aaa3177.

Gorbunova V, Seluanov A, Mita P, McKerrow W, Fenyö D, Boeke JD, Linker SB, Gage FH, Kreiling JA, Petrashen AP, *et al.* The role of retrotransposable elements in ageing and age-associated diseases. Nature. 2021;596(7870):43–53. doi:10.1038/s41586-021-03542-y.

Gramates LS, Agapite J, Attrill H, Calvi BR, Crosby MA, Dos Santos G, Goodman JL, Goutte-Gattat D, Jenkins VK, Kaufman T, *et al.* Fly base: a guided tour of highlighted features. Genetics. 2022;220(4):iyac035. doi:10.1093/genetics/iyac035.

Gundry M, Li W, Maqbool SB, Vijg J. Direct, genome-wide assessment of DNA mutations in single cells. Nucleic Acids Res. 2012;40(5):2032–2040. doi:10.1093/nar/gkr949.

Hancks DC, Kazazian HH Jr. 2016. Roles for retrotransposon insertions in human disease. Mob DNA. 7(1):9. doi:10.1186/s13100-016-0065-9.

Heigwer F, Port F, Boutros M. RNA interference (RNAi) screening in Drosophila. Genetics. 2018;208(3):853–874. doi:10.1534/genetics.117.300077.

Hoskins RA, Smith CD, Carlson JW, Carvalho AB, Halpern A, Kaminker JS, Kennedy C, Mungall CJ, Sullivan BA, Sutton GG, *et al.* Heterochromatic sequences in a Drosophila whole-genome shotgun assembly. Genome Biol. 2002;3(12):Research0085. doi:10.1186/gb-2002-3-12-research0085.

Hu Y, Comjean A, Rodiger J, Liu Y, Gao Y, Chung V, Zirin J, Perrimon N, Mohr SE. Flyrnai.org—the database of the Drosophila RNAi screening center and transgenic RNAi project: 2021 update. Nucleic Acids Res. 2020;49(D1):D908–D915. doi:10.1093/nar/gkaa936.

Hu Y, Comjean A, Roesel C, Vinayagam A, Flockhart I, Zirin J, Perkins L, Perrimon N, Mohr SE. Flyrnai.org-the database of the Drosophila RNAi screening center and transgenic RNAi project: 2017 update. Nucleic Acids Res. 2017;45(D1):D672–D678. doi:10.1093/nar/gkw977.

Hu Y, Flockhart I, Vinayagam A, Bergwitz C, Berger B, Perrimon N, Mohr SE. An integrative approach to ortholog prediction for disease-focused and other functional studies. BMC Bioinformatics. 2011;12(1):357. doi:10.1186/1471-2105-12-357.

Huang da W, Sherman BT, Lempicki RA. Systematic and integrative analysis of large gene lists using David bioinformatics resources. Nat Protoc. 2009;4(1):44–57. doi:10.1038/nprot.2008.211.

Hur JK, Luo Y, Moon S, Ninova M, Marinov GK, Chung YD, Aravin AA. Splicing-independent loading of trex on nascent RNA is required for efficient expression of dual-strand pirna clusters in Drosophila. Genes Dev. 2016;30(7):840–855. doi:10.1101/gad.276030.115.

Janssen A, Colmenares SU, Karpen GH. Heterochromatin: guardian of the genome. Annu Rev Cell Dev Biol. 2018;34(1):265–288. doi:10.1146/annurev-cellbio-100617-062653.

Jasienska G, Nenko I, Jasienski M. Daughters increase longevity of fathers, but daughters and sons equally reduce longevity of mothers. Am J Hum Biol. 2006;18(3):422–425. doi:10.1002/ajhb.20497.

Jawkar S, Nongthomba U. Indirect flight muscles in *Drosophila melanogaster* as a tractable model to study muscle development and disease. Int J Dev Biol. 2020;64(1–2–3):167–173. doi:10.1387/ijdb.190333un.

Josephson RK, Malamud JG, Stokes DR. Asynchronous muscle: a primer. J Exp Biol. 2000;203(18):2713–2722. doi:10.1242/jeb.203.18.2713.

Kalmykova AI, Klenov MS, Gvozdev VA. Argonaute protein piwi controls mobilization of retrotransposons in the Drosophila male germline. Nucleic Acids Res. 2005;33(6):2052–2059. doi:10.1093/nar/gki323.

Khor S, Cai D. Control of lifespan and survival by Drosophila nf-κb signaling through neuroendocrine cells and neuroblasts. Aging (Albany NY). 2020;12(24):24604–24622. doi:10.18632/aging.104196.

Kim D, Paggi JM, Park C, Bennett C, Salzberg SL. Graph-based genome alignment and genotyping with hisat2 and hisat-genotype. Nat Biotechnol. 2019;37(8):907–915. doi:10.1038/s41587-019-0201-4.

Klein JD, Qu C, Yang X, Fan Y, Tang C, Peng JC. C-fos repression by piwi regulates Drosophila ovarian germline formation and tissue morphogenesis. PLoS Genet. 2016;12(9):e1006281. doi:10.1371/journal.pgen.1006281.

Lander ES, Linton LM, Birren B, Nusbaum C, Zody MC, Baldwin J, Devon K, Dewar K, Doyle M, FitzHugh W, *et al.* Initial sequencing and analysis of the human genome. Nature. 2001;409(6822):860–921. doi:10.1038/35057062.

Levin HL, Moran JV. Dynamic interactions between transposable elements and their hosts. Nat Rev Genet. 2011;12(9):615–627. doi:10.1038/nrg3030.

Li H, Durbin R. Fast and accurate short read alignment with Burrows-Wheeler transform. Bioinformatics. 2009;25(14):1754–1760. doi:10.1093/bioinformatics/btp324.

Li H, Handsaker B, Wysoker A, Fennell T, Ruan J, Homer N, Marth G, Abecasis G, Durbin R. The sequence alignment/map format and samtools. Bioinformatics. 2009;25(16):2078–2079. doi:10.1093/bioinformatics/btp352.

Li D, Liu CM, Luo R, Sadakane K, Lam TW. Megahit: an ultra-fast single-node solution for large and complex metagenomics assembly via succinct de Bruijn graph. Bioinformatics. 2015;31-(10):1674–1676. doi:10.1093/bioinformatics/btv033.

Li W, Prazak L, Chatterjee N, Grüninger S, Krug L, Theodorou D, Dubnau J. Activation of transposable elements during aging and neuronal decline in Drosophila. Nat Neurosci. 2013;16(5):529–531. doi:10.1038/nn.3368.

Lin YR, Parikh H, Park Y. Stress resistance and lifespan enhanced by downregulation of antimicrobial peptide genes in the imd pathway. Aging (Albany NY). 2018;10(4):622–631. doi:10.18632/aging.101417.

López-Otín C, Blasco MA, Partridge L, Serrano M, Kroemer G. The hallmarks of aging. Cell. 2013;153(6):1194–1217. doi:10.1016/j.cell.2013.05.039.

Martin M, Hiroyasu A, Guzman RM, Roberts SA, Goodman AG. Analysis of Drosophila sting reveals an evolutionarily conserved antimicrobial function. Cell Rep. 2018;23(12):3537–3550.e6. doi:10.1016/j.celrep.2018.05.029.

Matsumoto N, Sato K, Nishimasu H, Namba Y, Miyakubi K, Dohmae N, Ishitani R, Siomi H, Siomi MC, Nureki O. Crystal structure and activity of the endoribonuclease domain of the pirna pathway factor maelstrom. Cell Rep. 2015;11(3):366–375. doi:10.1016/j.celrep.2015.03.030.

McCullers TJ, Steiniger M. Transposable elements in Drosophila. Mob Genet Elements. 2017;7(3):1–18. doi:10.1080/2159256X.2017.1318201.

Miao B, Fu S, Lyu C, Gontarz P, Wang T, Zhang B. Tissue-specific usage of transposable element-derived promoters in mouse development. Genome Biol. 2020;21(1):255. doi:10.1186/s13059-020-02164-3.

Miguel-Aliaga I, Jasper H, Lemaitre B. Anatomy and physiology of the digestive tract of *Drosophila melanogaster*. Genetics. 2018;210(2):357–396. doi:10.1534/genetics.118.300224.

Miller KN, Victorelli SG, Salmonowicz H, Dasgupta N, Liu T, Passos JF, Adams PD. Cytoplasmic DNA: sources, sensing, and role in aging and disease. Cell. 2021;184(22):5506–5526. doi:10.1016/j.cell.2021.09.034.

Myllymäki H, Valanne S, Rämet M. The Drosophila imd signaling pathway. J Immunol. 2014;192(8):3455–3462. doi:10.4049/jimmunol.1303309.

National Center for Health Statistics. Health, United States 2019. Hyattsville, MD: National Center for Health Statistics; 2021.

Oliveros JC. 2007–2015. Venny. An interactive tool for comparing lists with Venn's diagrams. https://bioinfogp.cnb.csic.es/tools/venny/index.html

Parekh VJ, Rathod VK, Pandit AB. 2.10—Substrate Hydrolysis: Methods, Mechanism, and Industrial Applications of Substrate Hydrolysis. In: Moo-Young M, editor. Comprehensive Biotechnology. 2nd ed. Burlington: Academic Press; 2011. p. 103–118.

Periquet G, Lemeunier F, Bigot Y, Hamelin MH, Bazin C, Ladevèze V, Eeken J, Galindo MI, Pascual L, Boussy I. The evolutionary genetics of the hobo transposable element in the *Drosophila melanogaster* complex. Genetica. 1994;93(1–3):79–90. doi:10.1007/BF01435241.

Perkins LA, Holderbaum L, Tao R, Hu Y, Sopko R, McCall K, Yang-Zhou D, Flockhart I, Binari R, Shim HS, *et al.* The transgenic RNAi project at Harvard Medical School: resources and validation. Genetics. 2015;201(3):843–852. doi:10.1534/genetics.115.180208.

Port F, Bullock SL. Augmenting crispr applications in Drosophila with tRNA-flanked sgrnas. Nat Methods. 2016;13(10):852–854. doi:10.1038/nmeth.3972.

Port F, Chen HM, Lee T, Bullock SL. Optimized crispr/cas tools for efficient germline and somatic genome engineering in Drosophila. Proc Natl Acad Sci U S A. 2014;111(29):E2967–E2976. doi:10.1073/pnas.1405500111.

Port F, Muschalik N, Bullock SL. 2015. Systematic evaluation of Drosophila crispr tools reveals safe and robust alternatives to autonomous gene drives in basic research. G3 (Bethesda). 5(7):1493–1502. doi:10.1534/g3.115.019083.

Port F, Starostecka M, Boutros M. Multiplexed conditional genome editing with cas12a in Drosophila. Proc Natl Acad Sci U S A. 2020a;117(37):22890–22899. doi:10.1073/pnas.2004655117.

Port F, Strein C, Stricker M, Rauscher B, Heigwer F, Zhou J, Beyersdörffer C, Frei J, Hess A, Kern K, *et al.* A large-scale resource for tissue-specific crispr mutagenesis in Drosophila. Elife. 2020b;9:e53865. doi:10.7554/eLife.53865.

Pray LA. Transposons: the jumping genes. Nature Education. 2008;1(1):204. https://www.nature.com/scitable/topicpage/transposons-the-jumping-genes-518/

Qiu S, Xiao C, Meldrum Robertson R. Different age-dependent performance in Drosophila wild-type canton-s and the white mutant w1118 flies. Comp Biochem Physiol A Mol Integr Physiol. 2017;206:17–23. doi:10.1016/j.cbpa.2017.01.003.

Quinlan AR, Hall IM. Bedtools: a flexible suite of utilities for comparing genomic features. Bioinformatics. 2010;26(6):841–842. doi:10.1093/bioinformatics/btq033.

Rigal J, Martin Anduaga A, Bitman E, Rivellese E, Kadener S, Marr MT. Artificially stimulating retrotransposon activity increases mortality and accelerates a subset of aging phenotypes in Drosophila. Elife. 2022;11:e80169. doi:10.7554/eLife.80169.

Scott EC, Gardner EJ, Masood A, Chuang NT, Vertino PM, Devine SE. A hot l1 retrotransposon evades somatic repression and initiates human colorectal cancer. Genome Res. 2016;26(6):745–755. doi:10.1101/gr.201814.115.

Shah D, Mital K. The role of trypsin:chymotrypsin in tissue repair. Adv Ther. 2018;35(1):31–42. doi:10.1007/s12325-017-0648-y.

Sherman BT, Hao M, Qiu J, Jiao X, Baseler MW, Lane HC, Imamichi T, Chang W. David: a web server for functional enrichment analysis and functional annotation of gene lists (2021 update). Nucleic Acids Res. 2022;50(W1):W216–W221. doi:10.1093/nar/gkac194.

Simon M, Van Meter M, Ablaeva J, Ke Z, Gonzalez RS, Taguchi T, De Cecco M, Leonova KI, Kogan V, Helfand SL, *et al.* Line1 derepression in aged wild-type and sirt6-deficient mice drives inflammation. Cell Metab. 2019;29(4):871–885.e5. doi:10.1016/j.cmet.2019.02.014.

Singh SH, Kumar P, Ramachandra NB, Nongthomba U. Roles of the troponin isoforms during indirect flight muscle development in Drosophila. J Genet. 2014;93(2):379–388. doi:10.1007/s12041-014-0386-8.

Sioud M. RNA interference: story and mechanisms. Methods Mol Biol. 2021;2282:1–15. doi:10.1007/978-1-0716-1298-9_1.

Siudeja K, van den Beek M, Riddiford N, Boumard B, Wurmser A, Stefanutti M, Lameiras S, Bardin AJ. 2021. Unraveling the features of somatic transposition in the Drosophila intestine. EMBO J. 40(9):e106388. doi:10.15252/embj.2020106388.

Smith CD, Shu S, Mungall CJ, Karpen GH. The release 5.1 annotation of *Drosophila melanogaster* heterochromatin. Science. 2007;316-(5831):1586–1591. doi:10.1126/science.1139815.

Szklarczyk D, Gable AL, Nastou KC, Lyon D, Kirsch R, Pyysalo S, Doncheva NT, Legeay M, Fang T, Bork P, *et al.* The string database in 2021: customizable protein-protein networks, and functional characterization of user-uploaded gene/measurement sets. Nucleic Acids Res. 2021;49(D1):D605–d612. doi:10.1093/nar/gkaa1074.

Valanne S, Wang JH, Rämet M. The Drosophila toll signaling pathway. J Immunol. 2011;186(2):649–656. doi:10.4049/jimmunol.1002302.

Vert JP, Foveau N, Lajaunie C, Vandenbrouck Y. An accurate and interpretable model for siRNA efficacy prediction. BMC Bioinformatics 2006;7:520

Vijg J, Suh Y. Genome instability and aging. Annu Rev Physiol. 2013; 75(1):645–668. doi:10.1146/annurev-physiol-030212-183715.

Wang JH, Valanne S, Rämet M. Drosophila As a model for antiviral immunity. World J Biol Chem. 2010;1(5):151–159. doi:10.4331/wjbc.v1.i5.151.

Ward JR, Khan A, Torres S, Crawford B, Nock S, Frisbie T, Moran JV, Longworth MS. Condensin I and condensin II proteins form a line-1 dependent super condensin complex and cooperate to repress line-1. Nucleic Acids Res. 2022;50(18):10680–10694. doi:10.1093/nar/gkac802.

Wood JG, Jones BC, Jiang N, Chang C, Hosier S, Wickremesinghe P, Garcia M, Hartnett DA, Burhenn L, Neretti N, *et al.* Chromatin-modifying genetic interventions suppress age-associated transposable element activation and extend life span in Drosophila. Proc Natl Acad Sci U S A. 2016;113(40):11277–11282. doi:10.1073/pnas.1604621113.

Yadav S, Eleftherianos I. Participation of the serine protease jonah66ci in the Drosophila antinematode immune response. Infect Immun. 2019;87(9):e00094-19. doi:10.1128/IAI.00094-19.

Yang N, Srivastav SP, Rahman R, Ma Q, Dayama G, Li S, Chinen M, Lei EP, Rosbash M, Lau NC. Transposable element landscapes in aging Drosophila. PLoS Genet. 2022;18(3):e1010024. doi:10.1371/journal.pgen.1010024.

Yu G, Wang LG, He QY. Chipseeker: an r/bioconductor package for chip peak annotation, comparison and visualization. Bioinformatics. 2015;31(14):2382–2383. doi:10.1093/bioinformatics/btv145.

Editor: M. Kuroda